J Therm Anal Calorim (2010) 102:1161–1166
DOI 10.1007/s10973-010-0808-7

Heat capacities and thermodynamic properties of one manganese-based MOFs

Li-Fang Song · Chun-Hong Jiang · Cheng-Li Jiao · Jian Zhang · Li-Xian Sun · Fen Xu · Qing-Zhu Jiao · Yong-Heng Xing · Yong Du · Zhong Cao · Feng-Lei Huang

Received: 25 February 2010 / Accepted: 13 April 2010 / Published online: 5 May 2010

Abstract A metal-organic framework $[Mn(4,4'\text{-bipy})(1,3\text{-BDC})]_n$ (MnMOF, 1,3-BDC = 1,3-benzene dicarboxylate, 4,4′-bipy = 4,4′-bipyridine) has been synthesized hydrothermally and characterized by single crystal XRD and FT-IR spectrum. The low-temperature molar heat capacities of MnMOF were measured by temperature-modulated differential scanning calorimetry for the first time. The thermodynamic parameters such as entropy and enthalpy relative to reference temperature 298.15 K were derived based on the above molar heat capacity data. Moreover, the thermal stability and the decomposition mechanism of MnMOF were investigated by thermogravimetry analysis-mass spectrometer. A two-stage mass loss was observed in air flow. MS curves indicated that the gas products of oxidative degradation were H_2O, CO_2, NO, and NO_2.

Keywords Manganese · Metal-organic framework · Molar heat capacity · TGA · TMDSC

L.-F. Song · C.-H. Jiang · C.-L. Jiao · J. Zhang · L.-X. Sun (✉)
Materials and Thermochemistry Laboratory, Dalian Institute of Chemical Physics, Chinese Academy of Sciences, 116023 Dalian, People's Republic of China
e-mail: lxsun@dicp.ac.cn

L.-F. Song · C.-H. Jiang · C.-L. Jiao
Graduate School of the Chinese Academy of Sciences, 100049 Beijing, People's Republic of China

F. Xu (✉) · Q.-Z. Jiao · Y.-H. Xing
Faculty of Chemistry and Chemical Engineering, Liaoning Normal University, 116029 Dalian, People's Republic of China
e-mail: xufen@lnnu.edu.cn

Y. Du
State Key Laboratory of Powder Metallurgy, Central South University, 410083 Changsha, People's Republic of China

Z. Cao
College of Chemistry and Biological Engineering, Changsha University of Science and Technology, 410076 Changsha, People's Republic of China

F.-L. Huang
State Key Laboratory of Explosion Science and Technology, Beijing Institute of Technology, 100081 Beijing, People's Republic of China

Introduction

Over the past decades, many metal-organic frameworks have been synthesized due to their diverse structural topologies and a variety of properties ranging from gas storage [1], catalysis [2], chemical sensor [3], separation [4], and biological analysis [5]. This class of materials can be easily obtained through self-assembly of metal ions as connected centers and organic ligands as linkers. The aromatic carboxylic acids and the bipyridine ligands are the most common polyfunctional organic linkers to form mixed-ligands frameworks [6]. The bipyridine ligands can combine different aromatic carboxylate co-ligands to assemble into diverse polymeric frameworks consisting of one-, two- or three-dimensional structures.

Molar heat capacities of the materials at different temperatures are basic data in chemistry and engineering, from which many other thermodynamic properties such as enthalpy and entropy can be calculated. These parameters are important for both theoretical and practical purposes. Heat capacities determinations of various compounds have been focused by many researchers. It is one of the most fundamental thermodynamic properties of substances and related to other physical and chemical properties closely.

Temperature-modulated differential scanning calorimetry (TMDSC) is one of the easier and more accurate

methods for determining the heat capacity. The structure and principle of the calorimeter have been described in detail by the literatures [7–10]. This method has been greatly developed for directly determining heat capacities for various materials nowadays [11, 12].

In this article, we reported one new mixed-ligands metal-organic framework. The low-temperature molar heat capacities of the compound were measured by TMDSC and the thermodynamic parameters such as entropy and enthalpy were also calculated. The accuracy of TMDSC was established by comparing the measured heat capacities of standard sapphire (Al_2O_3) with previously reported values (NIST and NBS) [13, 14]. The thermal decomposition characteristics of this compound were investigated by TGA-MS.

Experimental

All reagents were purchased commercially and used without further purification.

Sample preparation

$[Mn(4,4'\text{-bipy})(1,3\text{-BDC})]_n$ was prepared by hydrothermal reaction. A mixture of $Mn(CH_3COO)_2{\cdot}4H_2O$ (0.98 g, 4 mmol), 1,3-H_2BDC (0.66 g, 4 mmol), 4,4′-bipy (0.16 g, 1 mmol), and H_2O (20 mL) was sealed in a 40-mL Teflon-lined stainless steel autoclave and heated at 453 K for 4 days, then cooled to room temperature naturally. Yellow block crystals suitable to single crystal X-ray diffraction analysis were obtained in ca. 62% yield based on Mn(II). The product was washed with DMF after filtration and then dried at 323 K in vacuum overnight.

Characterization

The crystal data were collected at 293 K using a SMART APEX II-CCD single crystal XRD (graphite monochromated MoKα radiation, $\lambda = 0.71073$ Å). A multi-scan absorption correction was applied using the SADABS program. The structures were solved by direct methods and refined by full-matrix least-squares method implemented in SHELXTL-97 [15]. All the non-hydrogen atoms were refined anisotropically. Hydrogen atoms were added theoretically. FT-IR spectra were recorded on a Nicolet 380 FT-IR spectrometer using KBr pellet in the wavenumber range of 4000–400 cm^{-1}.

Crystal data for the MnMOF were as follows: triclinic system, *P-1* (no. 2), $a = 9.056(11)$ Å, $b = 9.933(12)$ Å, $c = 10.135(13)$ Å, $\alpha = 79.550(19)°$, $\beta = 74.26(2)°$, $\gamma = 74.86(2)°$. The molar mass is 375.24 g mol^{-1}. Mn(II) center is located in a six-coordinated slightly distorted octahedral environment, being surrounded by four carboxylate oxygen atoms from three 1,3-BDC ligands and two pyridyl nitrogens from a pair of 4,4′-bipyridine. The distances of Mn–O are 2.082(9), 2.119(9), 2.206(9), and 2.274(3) Å. The distances of Mn–N are 2.284(11) and 2.095(12) Å. The O(N)–Mn–O(N) bond angles vary from 57.7(3) to 176.4(4)°.

The IR spectrum is shown in Fig. 1. The broad absorption band centered at 3427 cm^{-1} shows the presence of hydrogen-bonding interactions in the framework. The weak absorption band at 3058 cm^{-1} is caused by ν(C–H) (phen) stretching vibrations. The existence of two very strong bands at 1569 and 1396 cm^{-1}, attributed to the ν_{as}(OCO) and ν_s(OCO) stretching vibrations of the 1,3-BDC ligand. Characteristic vibrations of aromatic nucleus [ν(C–C), ν(C–N)] are near 1604 and 1546 cm^{-1}, while ν(C–H) deformation vibrations are about 811 and 720 cm^{-1} (phen).

Heat capacity measurement

Heat capacity measurements of the MnMOF were performed on a DSC Q1000 (T-zero DSC-technology, TA Instruments Inc., USA). A mechanical cooling system was used for the experimental measurement. Dry nitrogen gas with high purity (99.999%) was used as purge gas (50 mL min^{-1}) through the DSC cell. The temperature scale of the instrument was initially calibrated in the standard DSC mode, using the extrapolated onset temperatures of the melting of indium (429.75 K) at a heating rate of 10 K min^{-1}. The energy scale was calibrated with the heat of fusion of indium (28.45 J g^{-1}). The heat capacity calibration was made by running a standard sapphire (α-Al_2O_3) at the experimental temperature. The calibration method was performed at the conditions as follows: (1) sampling interval: 1.00 s/pt; (2) zero heat flow at 328.15 K; (3) equilibrate at 183.15 K; (4) isothermal for

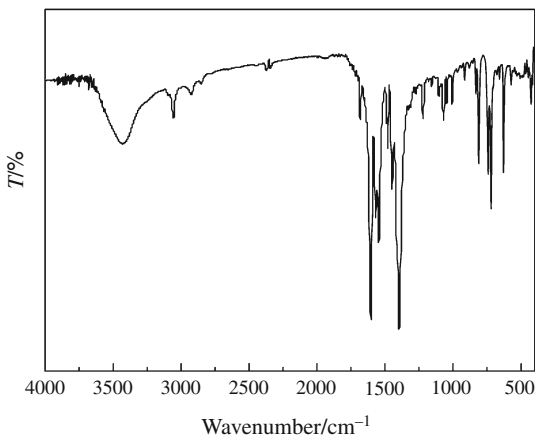

Fig. 1 IR spectrum of MnMOF

5.00 min; (5) temperature ramp at 10 K min^{-1} to 473.15 K.

Samples were crimped in hermetically sealed aluminum pans with lids using TA's Blue DSC Sample Press. Sample mass was weighed on a METTLER TOLEDO analytical balance (AB135-S, Classic Plus). The masses of the reference and sample pans with lids were within 54.25 ± 0.05 mg.

Thermal analysis

Thermogravimetric analysis (TGA) was carried out on a Cahn Thermax 500 from 290 to 1073 K. The heating rate was 10 K min^{-1} and the flow rate of air was 100 mL min^{-1}. The mass of the MnMOF was 55.63 mg. The TG equipment was calibrated by the $CaC_2O_4{\cdot}H_2O$ (99.9%). Mass spectra (MS) were performed on a Multi-component Online Gas Analyzer GAM 200.

Results and discussion

Heat capacity of standard sapphire (α-Al_2O_3)

Heat capacity measurements were repeated three times unless stated elsewhere. The emphasis of this work is to assess the reproducibility and ensure accuracy of the measured data using TMDSC (Q1000). The experimental standard deviation is during ±0.0016 and the result shows that the testing system of TMDSC is steady. Relative deviations have been calculated by the following equation:

$$\mathrm{RD}\,(\%) = 100\left[C_{p,\mathrm{m}}(\mathrm{exp}) - C_{p,\mathrm{m}}(\mathrm{ref})\right]/C_{p,\mathrm{m}}(\mathrm{ref}) \qquad (1)$$

where $C_{p,\mathrm{m}}$(exp) is the average experimental heat capacities and $C_{p,\mathrm{m}}$(ref) is the referenced heat capacities. The results show that the relative deviation of our calibration data from the recommended value [13] was within ±2.2% over the whole temperature range.

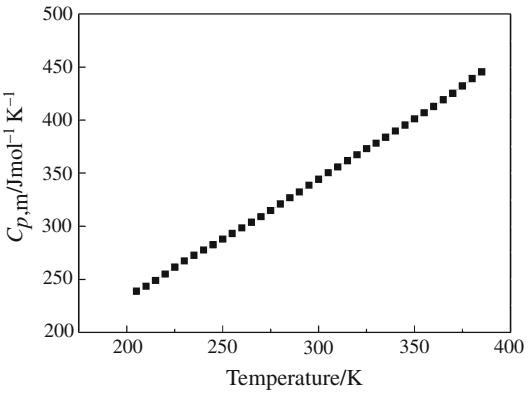

Fig. 2 Molar heat capacities ($C_{p,\mathrm{m}}$) of MnMOF as a function of temperature

Heat capacity of MnMOF

The average experimental molar heat capacities curve of MnMOF versus temperature is shown in Fig. 2. It can be seen that the heat capacity of the sample increases with increasing temperature continuously in the temperature

Table 1 The data of three reduplicate experiments for MnMOF

T/K	$C_{p,\mathrm{m}}$(exp)/J K^{-1} g^{-1}				Standard deviation
	a	*b*	*c*	Average	
205	0.6365	0.6353	0.6376	0.6365	0.0012
210	0.6493	0.6474	0.6497	0.6488	0.0012
215	0.6639	0.6622	0.6641	0.6634	0.0010
220	0.6795	0.6786	0.6803	0.6795	0.0009
225	0.6971	0.6956	0.6977	0.6968	0.0011
230	0.7129	0.7109	0.7135	0.7124	0.0014
235	0.7268	0.7253	0.7275	0.7265	0.0011
240	0.7405	0.7386	0.7409	0.7400	0.0012
245	0.7537	0.7514	0.7548	0.7533	0.0017
250	0.7672	0.7658	0.7686	0.7672	0.0014
255	0.7811	0.7801	0.7830	0.7814	0.0015
260	0.7949	0.7945	0.7974	0.7956	0.0016
265	0.8094	0.8085	0.8113	0.8097	0.0014
270	0.8234	0.8222	0.8251	0.8236	0.0015
275	0.8393	0.8379	0.8404	0.8392	0.0013
280	0.8556	0.8539	0.8570	0.8555	0.0016
285	0.8708	0.8702	0.8725	0.8712	0.0012
290	0.8857	0.8847	0.8874	0.8859	0.0014
295	0.9010	0.9021	0.9049	0.9027	0.0020
300	0.9168	0.9171	0.9193	0.9177	0.0014
305	0.9322	0.9329	0.9357	0.9336	0.0019
310	0.9465	0.9480	0.9504	0.9483	0.0020
315	0.9621	0.9638	0.9660	0.9640	0.0020
320	0.9771	0.9788	0.9805	0.9788	0.0017
325	0.9924	0.9937	0.9956	0.9939	0.0016
330	1.0060	1.0080	1.0090	1.0077	0.0015
335	1.0220	1.0220	1.0240	1.0227	0.0012
340	1.0370	1.0380	1.0400	1.0383	0.0015
345	1.0530	1.0530	1.0540	1.0533	0.0006
350	1.0690	1.0680	1.0700	1.0690	0.0010
355	1.0850	1.0840	1.0840	1.0843	0.0006
360	1.1010	1.1000	1.1000	1.1003	0.0006
365	1.1180	1.1160	1.1170	1.1170	0.0010
370	1.1340	1.1330	1.1330	1.1333	0.0006
375	1.1530	1.1510	1.1510	1.1517	0.0012
380	1.1710	1.1710	1.1690	1.1703	0.0012
385	1.1890	1.1870	1.1850	1.1870	0.0020

Table 2 The experimental and simulated molar heat capacities of MnMOF

T/K	$C_{p,m}$(exp)/ J K^{-1} mol^{-1}	$C_{p,m}$(fit)/ J K^{-1} mol^{-1}	RD (%)	T/K	$C_{p,m}$(exp)/ J K^{-1} mol^{-1}	$C_{p,m}$(fit)/ J K^{-1} mol^{-1}	RD (%)
205	238.8	237.9	−0.38	300	344.4	344.1	−0.09
210	243.5	244.1	0.27	305	350.3	237.9	−0.38
215	248.9	250.0	0.43	310	355.8	244.1	0.27
220	255.0	255.7	0.28	315	361.7	250.0	0.43
225	261.5	261.2	−0.11	320	367.3	255.7	0.28
230	267.3	266.6	−0.28	325	373.0	261.2	−0.11
235	272.6	271.9	−0.26	330	378.1	266.6	−0.28
240	277.7	277.2	−0.16	335	383.7	271.9	−0.26
245	282.7	282.6	−0.04	340	389.6	390.7	0.28
250	287.9	287.9	0.01	345	395.3	396.7	0.38
255	293.2	293.3	0.03	350	401.1	402.8	0.41
260	298.5	298.7	0.07	355	406.9	408.8	0.46
265	303.8	304.2	0.13	360	412.9	414.8	0.46
270	309.0	309.8	0.25	365	419.1	420.7	0.38
275	314.9	315.4	0.16	370	425.3	426.7	0.33
280	321.0	321.1	0.02	375	432.2	432.6	0.10
285	326.9	326.8	−0.03	380	439.2	438.5	−0.16
290	332.4	332.5	0.03	385	445.4	444.3	−0.25
295	338.7	338.3	−0.12				

Table 3 Calculated thermodynamic function data of MnMOF

T/K	$H_T - H_{298.15}$/ kJ mol^{-1}	$S_T - S_{298.15}$/ J K^{-1} mol^{-1}	T/K	$H_T - H_{298.15}$ / kJ mol^{-1}	$S_T - S_{298.15}$/ J K^{-1} mol^{-1}
205	−27.01	−107.45	298.15	0	0
210	−25.80	−101.63	300	0.64	2.13
215	−24.57	−95.82	305	2.37	7.86
220	−23.30	−90.01	310	4.13	13.60
225	−22.01	−84.20	315	5.93	19.34
230	−20.69	−78.40	320	7.75	25.08
235	−19.34	−72.61	325	9.60	30.81
240	−17.97	−66.83	330	11.48	36.55
245	−16.57	−61.05	335	13.38	42.29
250	−15.14	−55.28	340	15.32	48.03
255	−13.69	−49.53	345	17.28	53.76
260	−12.21	−43.78	350	19.27	59.50
265	−10.70	−38.03	355	21.29	65.23
270	−9.17	−32.29	360	23.34	70.97
275	−7.61	−26.55	365	25.42	76.71
280	−6.02	−20.81	370	27.53	82.45
285	−4.40	−15.08	375	29.68	88.20
290	−2.75	−9.34	380	31.85	93.97
295	−1.07	−3.61	385	34.06	99.75

range from 205 to 385 K. No phase transition or thermal anomaly was observed in the experimental temperature range. This indicates that the sample is stable in this temperature region.

The data of three reduplicate experiments and the experimental standard deviation for MnMOF are given in Table 1. The experimental standard deviations below 0.0020 are obtained and show reasonably good

reproducibility. The experimental and simulated molar heat capacities data are listed in Table 2.

The molar heat capacities of the sample are fitted to the following polynomial equation of heat capacities ($C_{p,\mathrm{m}}$) with reduced temperature (X) using the OriginPro 7.5 software:

From T = (205 to 385) K

$$C_{p,\mathrm{m}}\left(\mathrm{J\ mol^{-1}K^{-1}}\right) = 338.3 + 103.9\mathrm{X} + 1.807\mathrm{X}^2 - 10.59^3 + 1.863\ \mathrm{X}^4 + 10.74\ \mathrm{X}^5 \quad (2)$$

where $X = (T - 295)/90$ and T is the experimental temperature, 295 is obtained from polynomial $(T_{\max} + T_{\min})/2$, 90 is obtained from polynomial $(T_{\max} - T_{\min})/2$, $T_{\max}$ is the upper limit (385 K) of the above temperature region, $T_{\min}$ is the lower limit (205 K) of the above temperature region. The correlation coefficient is $R^2 = 0.99995$. The relative deviations of all the experimental points from the fitting heat capacities values are within ±0.46%. Based on Eq. 2, the molar heat capacity of the sample at 298.15 K was calculated to be 341.9 J mol^{-1} K^{-1}.

Thermodynamic functions of MnMOF

Enthalpy and entropy of substances are basic thermodynamic functions. In terms of the polynomials of molar heat capacity and the thermodynamic relationship, the $[H_T - H_{298.15}]$ and $[S_T - S_{298.15}]$ of MnMOF are calculated with an interval of 5 K relative to the temperature of 298.15 K. The thermodynamic relationships are as follows:

$$H_T - H_{298.15} = \int_{298.15}^{T} C_{p,\mathrm{m}}\,\mathrm{d}T \quad (3)$$

$$S_T - S_{298.15} = \int_{298.15}^{T} \left(C_{p,\mathrm{m}}/T\right)\mathrm{d}T \quad (4)$$

The calculated thermodynamic functions $[H_T - H_{298.15}]$ and $[S_T - S_{298.15}]$ are shown in Table 3.

Thermal stability and decomposition of MnMOF

TG curve (Fig. 3) of MnMOF shows a two-stage mass loss in the temperature range from 290 to 1073 K. The first mass loss starts at about 390 K and is about 8.40%, the MS curve (Figs. 4, 5) shows that the decomposed products are mainly H_2O (m/z = 18) and NO (m/z = 30), which is due to the decomposition of part of the 4,4′-bipyridine ligands. Further decomposition occurs in the region of 709 to 823 K according to the degradation of the 1,3-BDC and 4,4′-bipyridine ligands, which means the degradation of the framework. The MS curve (Figs. 4, 5) shows that the gas degradation products in this stage are mainly H_2O (m/z = 18), CO_2 (m/z = 12, 44), NO (m/z = 30) and NO_2 (m/z = 30, 46). The overall mass loss of the sample is about 77.8% in accord with the calculated percentage (79.7), which indicates that the sample was probably decomposed to the Mn_3O_4.

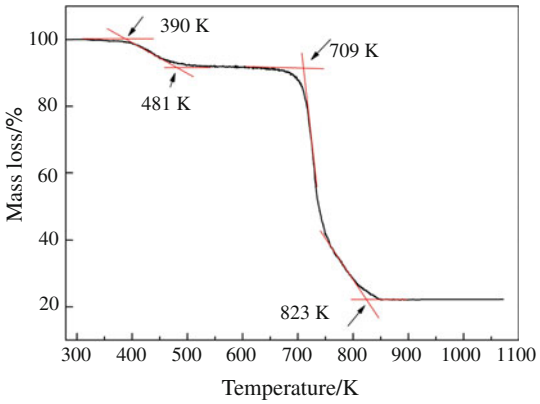

Fig. 3 TG curves of MnMOF

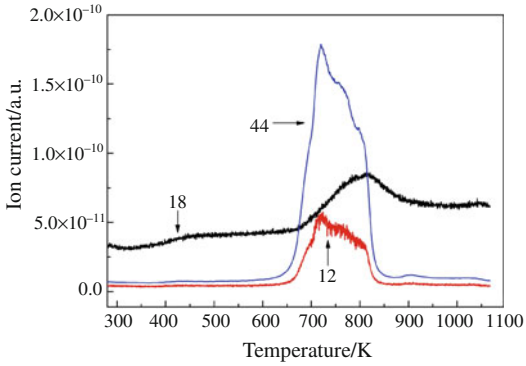

Fig. 4 MS curves (m/z = 12, 18, 44)

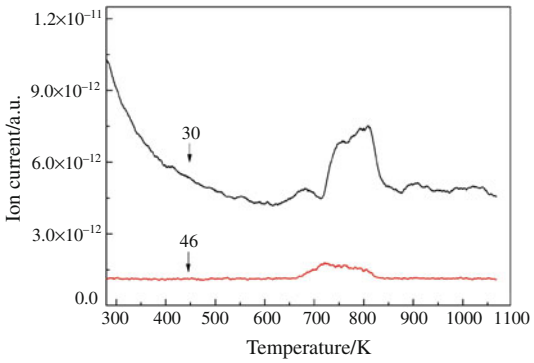

Fig. 5 MS curves (m/z = 30, 46)

Conclusions

In this study, one new mixed-ligands metal-organic framework has been synthesized and characterized by single crystal X-ray diffraction and FT-IR spectrum. The molar heat capacities of the compound were measured using TMDSC for the first time. The heat capacity of the sample at 298.15 K was calculated to be 341.9 J mol^{-1} K^{-1}. The thermodynamic function data relative to the reference temperature (298.15 K) were calculated based on the heat capacities measurements. Moreover, the thermal stability of the compound was further investigated by TGA-MS.

Acknowledgments The authors gratefully acknowledge the financial support for this study from the National Natural Science Foundation of China (Nos. 20833009, 20873148, 20903095, 50901070, and U0734005), the National Basic Research Program (973 program) of China (2010CB631303), IUPAC (Project No. 2008-006-3-100), Dalian Scientific Project (2009A11GX052), and the State Key Laboratory of Explosion Science and Technology, Beijing Institute of Technology (Grant No. KFJJ10-1Z).

References

1. Murray LJ, Dinca M, Long JR. Hydrogen storage in metal-organic frameworks. Chem Soc Rev. 2009;38:1294–314.
2. Lee J, Farha OK, Roberts J, Scheidt KA, Nguyen ST, Hupp JT. Metal-organic framework materials as catalysts. Chem Soc Rev. 2009;38:1450–9.
3. Liu YY, Zhang J, Xu F, Sun LX, Zhang T, You WS, et al. Lithium-based 3D coordination polymer with hydrophilic structure for sensing of solvent molecules. Cryst Growth Des. 2008;8:3127–9.
4. Bae YS, Mulfort KL, Frost H, Ryan P, Punnathanam S, Broadbelt LJ, et al. Separation of CO_2 from CH_4 using mixed-ligand metal-organic frameworks. Langmuir. 2008;24:8592–8.
5. Contreras R, Flores-Parra A, Mijangos E, Tellez F, Lopez-Sandoval H, Barba-Behrens N. From mono to polydentate azole and benzazole derivatives, versatile ligands for main group and transition metal atoms. Coordin Chem Rev. 2009;253:1979–99.
6. Kumar DK, Das A, Dastidar P. One-dimensional chains, two-dimensional corrugated sheets having a cross-linked helix in metal-organic frameworks: exploring hydrogen-bond capable backbones and ligating topologies in mixed ligand systems. Cryst Growth Des. 2006;6:1903–9.
7. Reading M, Luget A, Wilson R. Modulated differential scanning calorimetry. Thermochim Acta. 1994;238:295–307.
8. Wunderlich B, Jin YM, Boller A. Mathematical-description of differential scanning calorimetry based on periodic temperature modulation. Thermochim Acta. 1994;238:277–93.
9. Wunderlich B. The contributions of MDSC to the understanding of the thermodynamics of polymers. J Therm Anal Calorim. 2006;85:179–87.
10. Danley RL. New modulated DSC measurement technique. Thermochim Acta. 2003;402:91–8.
11. Qiu SJ, Chu HL, Zhang J, Qi YN, Sun LX, Xu F. Heat capacities and thermodynamic properties of CoPc and CoTMPP. J Therm Anal Calorim. 2008;91:841–8.
12. Zhang J, Liu YY, Zeng JL, Xu F, Sun LX, You WS, et al. Thermodynamic properties and thermal stability of the synthetic zinc formate dihydrate. J Therm Anal Calorim. 2008;91:861–6.
13. Archer DG. Thermodynamic properties of synthetic sapphire (Alpha-Al_2O_3), standard reference material 720 and the effect of temperature-scale differences on thermodynamic properties. J Phys Chem Ref Data. 1993;22:1441–53.
14. Ginnings DC, Furukawa GT. Heat capacity standards for the range 14-Degrees-K to 1200-Degrees-K. J Am Chem Soc. 1953;75:522–7.
15. Sheldrick GM. SHELX97, Program for crystal structure refinement. Germany: Göttingen University; 1997.